Unusual heterocyclization of chalcone podands with 3-amino-1,2,4-triazole

I. G. Ovchinnikova, M. S. Valova, E. G. Matochkina, M. I. Kodess, A. A. Tumashov, P. A. Slepukhin, O. V. Fedorova, G. L. Rusinov, and V. N. Charushin*

I. Ya. Postovsky Institute of Organic Synthesis, Ural Branch of the Russian Academy of Sciences, 22/20 ul. S. Kovalevskoi, 620041 Ekaterinburg, Russian Federation. Fax: +7 (343) 374 1189. E-mail: iov@ios.uran.ru

A new type of intramolecular cyclization of 1,5-bis[2-(*E*-3-oxo-3-phenylprop-1-enyl)-phenoxy]-3-oxapentane with 3-aminotriazole promoted by potassium ions was discovered. A cascade mechanism for the formation of crownophane with 4,7-dihydro[1,2,4]triazolo[1,5-*a*]-pyrimidine fragment was suggested. Effects of oligooxyethylene fragment of the chalcone podand and acid-base catalysis on the selectivity of the cyclocondensation processes and degree of oxidation of triazolopyrimidine fragments were studied. The product structures were confirmed by IR, ^{1}H and ^{13}C NMR spectroscopy and X-ray diffraction study.

Key words: template synthesis, chalcone podand, crown ethers, cascade reaction, heterocyclization, 1,2,4-triazolo[1,5-*a*]pyrimidine-containing podands.

Azolopyrimidines with the nodal nitrogen atom, including 1,2,4-triazolo[1,5-*a*]pyrimidines and their dihydro derivatives, synthetic analogs of purines and nucleosides, exhibit a wide range of biological activity.[1—7] In addition, these compounds tend to form fairly stable complexes with metal ions.[8—12]

Incorporation of an oligooxyethylene fragment into azolopyrimidines and preparation of the open-chain analogs of crown ethers (podands) can be of certain interest for medicinal chemistry, since it is known that podands can mimic behavior of natural ionophores (for example, nihericine), performing transportation function in living cells.[13]

One of the most convenient methods for functionalization of podands with azolopyrimidine moieties consists in cyclocondensation of α,β-unsaturated carbonyl compounds (chalcones) with aminoazoles, in particular, with 3-amino-1,2,4-triazole. A number of works[14—23] thoroughly studied effects of the nature of solvents, catalysts, and substituents in both aminoazoles and chalcones on regioselectivity of the reactions leading to the formation of azoloazines. It was found that electron-donating substituents at position 5 of the dihydroazolopyrimidine system significantly affect the imino-enamine tautomerism of the heterocycle.[14,21] However, there is virtually no data on the influence of *ortho*-substituents (in particular, alkoxy groups) in the aromatic ring of chalcone cinnamoyl fragments on the selectivity of formation of cyclocondensation products with aminoazoles. For podands[24,25] with bulky oligooxyethylene fragment, such an influence can be significant. For instance, earlier it was shown that oligoethers with terminal 2-formylaryl groups can be involved into the three-component Biginelly reaction with aminoazoles and ethyl acetoacetate to form expected bis-dihydroazolopyrimidine derivatives.[26] At the same time, attempted preparation of analogous bis-1,4-dihydropyridine polyether systems in the Ganch reaction led to γ-piperidone-containing crownophanes.[27,28] Unusual ability to be converted to macrocyclic structures as a result of photochemical transformations or reactions with binucleophiles was found for chalcone podands as well.[25,29]

In the present work, we studied reactions of the earlier synthesized chalcone podand **1** with 3-amino-1,2,4-triazole and considered effect of the acid-base catalysis and solvent on the selectivity of chemical transformations.

Results and Discussion

The reaction of aminotriazole **2** with chalcone podand **1** in DMF at 75—80 °C leads to the formation of four major cyclocondensation products **4**—**7** (Scheme 1, Table 1).

The ^{1}H NMR spectroscopic data of the reaction mixtures indicate the formation of podands **3**—**6** and crownophane **7** with 1,2,4-triazolo[1,5-*a*]pyrimidine fragment, that confirms the earlier[14—21] established fact on regiospecificity of the cyclocondensation process of 3-amino-1,2,4-triazole with chalcones. The ^{1}H NMR spectra of symmetric podands **4** and **6** are characterized[19,21] by the singlet signals for the protons at the C(2) carbon atom of the triazole and C(6) carbon atom of the pyrimidine rings at δ 8.55 and 7.93, respectively, whereas the unsymmetric podand **5** shows them at δ 8.56 and 7.96, respectively. Introduction of the hydroxy group at position 6 of the pyrimidine ring (compounds **5** and **6**) leads to the upfield shift of

Published in Russian in *Izvestiya Akademii Nauk. Seriya Khimicheskaya,* No. 5, pp. 941—950, May, 2011.

Scheme 1

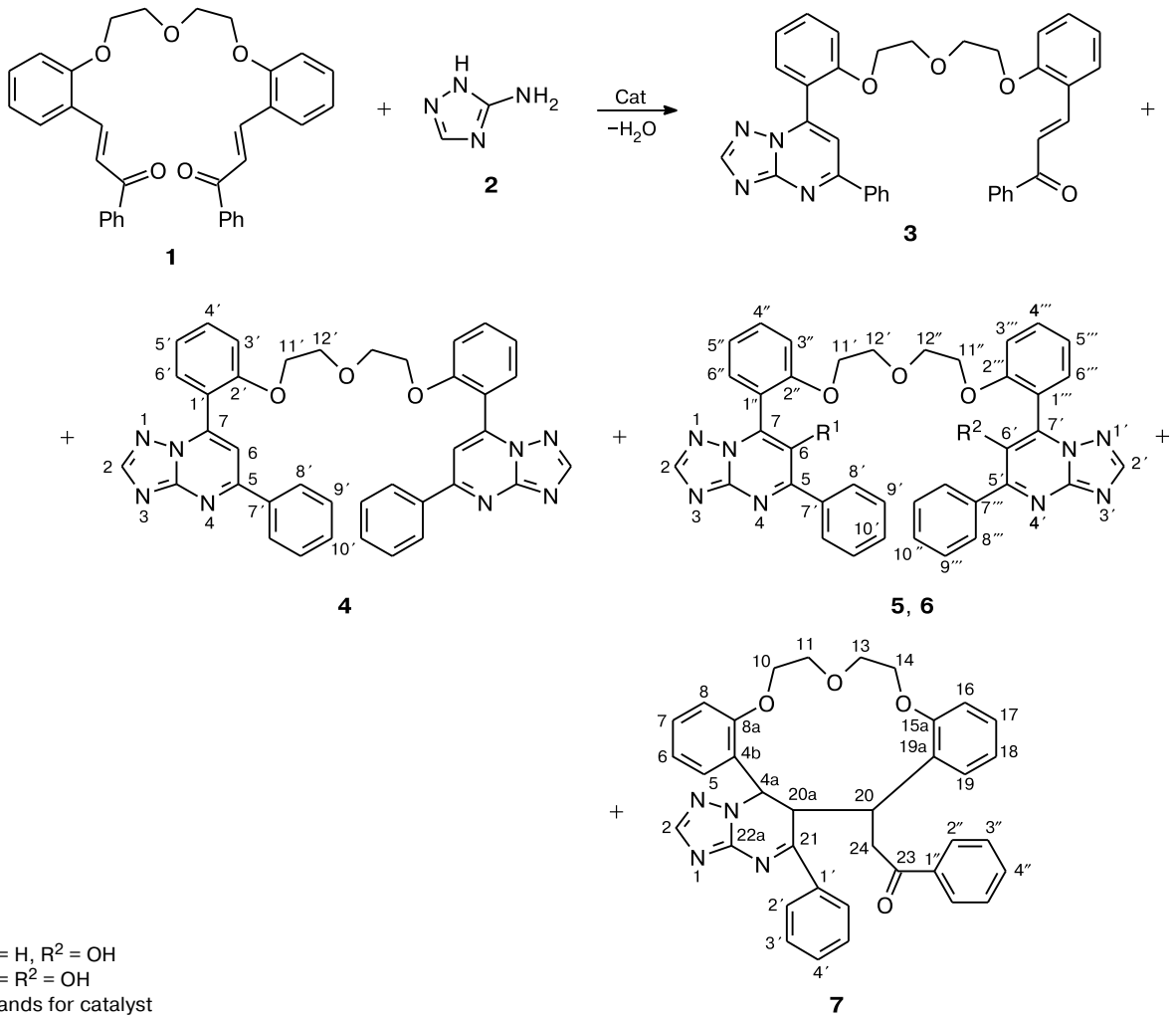

5: R^1 = H, R^2 = OH
6: R^1 = R^2 = OH
Cat stands for catalyst

the signal for the proton at the C(2) carbon atom by about 0.2 ppm.

The reaction of aminoazoles with chalcones usually stops at the step of formation of dihydroazolopyrimidines.[14] For podands, the process is finished by aromatization with the formation of products **4**—**6**, with their ratios in the reaction mixtures being significantly dependent on the catalyst (see Table 1). For instance, a predominant formation of podand **4** was observed in the presence of KOH, while in other cases the equilibrium was displaced to the side of 6-oxy-substituted 1,2,4-triazolo[1,5-*a*]pyrimidine podands **5** and **6**. Ability of dihydroazolopyrimidines to aromatization upon the action of air oxygen in the reaction mixtures to form 6-oxy-substituted derivatives is more pronounced in dihydropyrazolo[1,5-*a*]pyrimidines and dihydropyrimido[1,2-*a*]benzimidazoles.[14,22] Conversely, for dihydrotriazolo[1,5-*a*]pyrimidines due to the effects of several aza groups, such an oxidation process proceeded predominantly in the alkali alcoholic solutions.[17] In our studies, the presence of 6-oxy-substituted products was found in all the reaction mixtures independent on the medium pH.

Table 1. Results of the reaction of chalcone podand **1** with aminotriazole **2** according to the HPLC data

Entry	Catalyst	Solvent	Yield (%)				
			1 + **3***	**4**	**5**	**6**	**7**
1	KOH	EtOH	2	53	12	10	18
2	KOH	DMF	6	74	4	3	12
3	Et_3N	DMF	6	50	25	12	7
4	—	DMF	2	35	42	11	6
5	HCl	DMF	4	19	50	22	4

* A mixture of the starting (**1**) and monosubstituted triazolopyrimidine podands (**3**) according to the ^{1}H NMR spectra of the reaction mixtures.

The X-ray diffraction data on the crystals of triazolopyrimidine podands shows not only the structural,

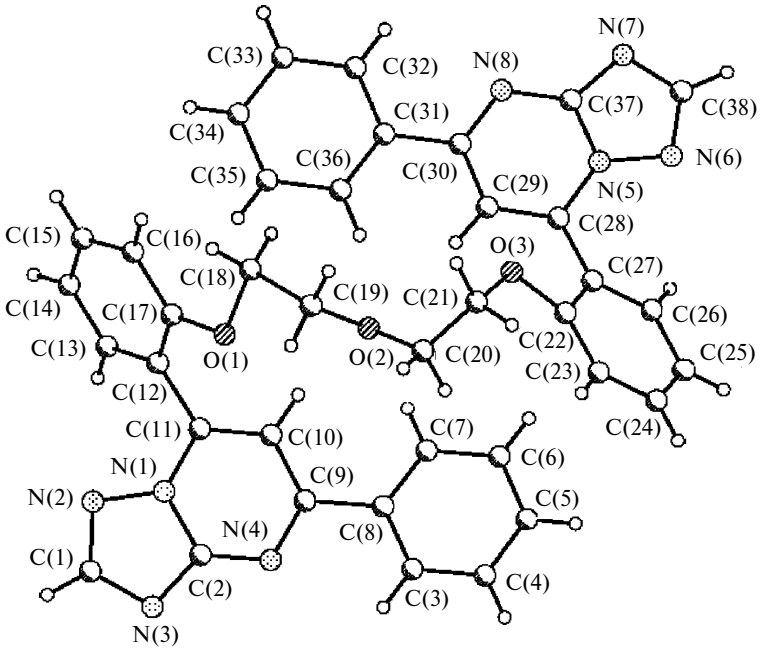

Fig. 1. Molecular geometry of 1,2,4-triazolo[1,5-*a*]pyrimidine podand **4**.

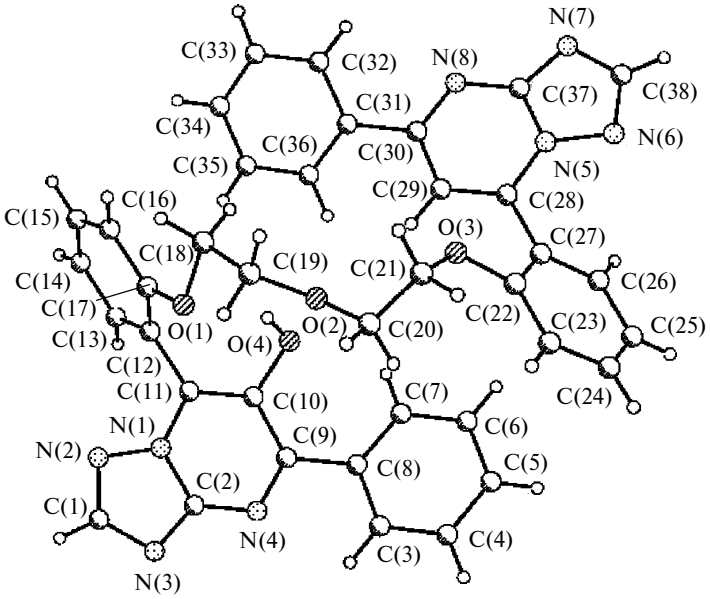

Fig. 2. Molecular geometry of 1,2,4-triazolo[1,5-*a*]pyrimidine podand **5**.

but also conformational similarities of the molecules (Fig. 1—3).

Molecules of symmetric podands **4** and **6**, which like compound **5** formally are related to the group of compounds with the C_2 symmetry, in crystals have the C_1 symmetry. For any of the three podands **4**—**6**, both the right and the left spiral-like direction of the oligooxyethylene fragments is observed, set by the same conformational sequence a—$g^{(+)}$—a—$g^{(-)}$—$g^{(-)}$—$g^{(-)}$ or a—$g^{(-)}$—a—$g^{(+)}$—$g^{(+)}$—$g^{(+)}$ of their units (see Fig. 1—3 and Ref. 30). In particular, for podand **6** the absolute values of torsional angles C(17)O(1)C(18)C(19), O(1)C(18)C(19)O(2), C(18)C(19)O(2)C(20), C(19)O(2)C(20)C(21), O(2)C(20)C(21)O(3), and C(20)C(21)O(3)C(22) are equal to 168.0, 63.6, 178.1, 86.5, 67.6, and 85.5°, respectively. Such a spatial geometry of molecules in crystals has been also found earlier for chalcone podands[24,25] (for example, for compound **1**).

In addition, in molecules **4**—**6** all the aromatic substituents of the terminal groups are arranged in different planes

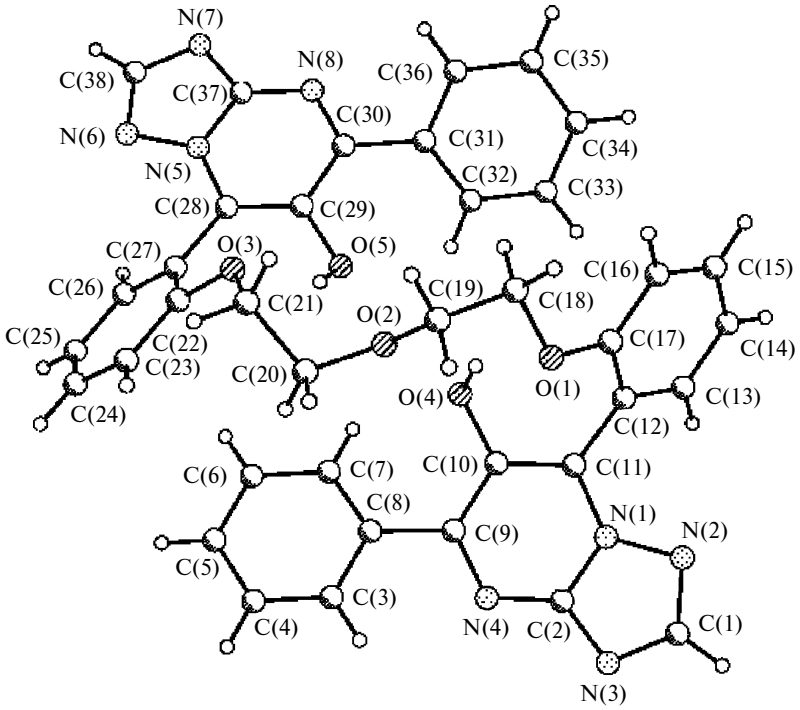

Fig. 3. Molecular geometry of 1,2,4-triazolo[1,5-*a*]pyrimidine podand **6**.

with respect to each other. For example, the phenyl substituents C(12)—C(17)/C(7)—C(8) and C(22)—C(27)/C(31)—C(32) are turned from the plane of C(10)—C(11) and C(29)—C(30) azoloazine rings, respectively, by the angles 45.2/33.1° and 47.0/27.3° for compound **4**, 48.6/31.3° and 48.0/34.9° for compound **5**, and 50.7/30.4° and 47.4/38.4° for compound **6**.

For compounds **4** and **5**, the X-ray diffraction study at 295(2) K established that the conformationally labile oligooxyethylene fragment is disordered. The disordering of the polyether chain of the crown ether molecules and their acyclic analogs in crystals is a frequent enough phenomenon, if the X-ray diffraction studies are performed at room temperature. The trioxydiethylene fragment in podand **4** is disordered over two positions with the population coefficient 0.5. In compound **5**, position of the OH group is disorder over two positions with the population coefficients 0.5, and a flexible chain of the polyether fragment is also disordered. However, unlike **4**, positions of the bridged oxygen atoms O(1) and O(3) are stabilized due to the specific interactions with the hydroxy group of the azinoazole ring. The distances O(4)—H...O(1) and O(4)—H...O(2) for podands **4** and **5** are equal to 1.89 and 2.46 Å (2.48 and 1.93 Å for the polyether fragment in the second position), respectively. The fact that such interactions arise and are able to affect lability of the oligooxyethylene fragment is confirmed by the structure of compound **6**, in which this fragment is not disordered, whereas the bridged oxygen atoms are fixed in positions corresponding to the geometry of intramolecular hydrogen bonds (IMHB) of the type O—H...O with the hydroxy groups of azoloazines. The hydrogen bond has the following parameters: the distances O(4)—H...O(1) and O(4)—H...O(2) are equal to 2.00 and 2.38 Å, whereas the distances O(5)—H...O(3) and O(5)—H...O(2) are equal to 1.93 and 2.51 Å, respectively.

Podands **4**—**6** due to their conformational specificities can be related to the group of compounds with the axial and planar chirality.[31—33] According to the X-ray diffraction data, the spiral character of molecules of these compounds (see Fig. 1—3) can be due to both the axial chirality (because of hindered rotation around simple C—C bonds of the sp^2—sp^2-type between the bulky bridged aryl and triazolopyrimidine substituents) and the planar chirality (because of stabilization of the synclinal conformation of the oxyethylene units, which provides the spiral-like geometry of the polyether fragment). It is known that significant conformational differences in such compounds, helicates and atropoisomers,[31—33] can lead to diastereotopic effect of substituents, which can be registered by NMR spectroscopy. Thus, if for compound **4** this effect is leveled in solutions, that is seen from the "symmetric" ^{1}H and ^{13}C NMR spectra, then for podand **6** the picture is quite the opposite. The differences in the conformation parameters of the oligooxyethylene fragment and terminal groups in podand **6** are preserved in solution, by all accounts, due to the bifurcated IMHB of the hydrogen atoms of OH groups with the bridged oxygen atoms of the polyether fragment. This phenomenon can be the reason for the "unsymmetry" of the ^{1}H and ^{13}C NMR spectra. In

fact, the ^{1}H NMR spectra of compound **6** obtained at 22 °C exhibit two singlets for the protons at the carbon atoms C(2) and C(2′) of the azole rings at δ 8.38 and 8.36 and two singlets for the protons of the OH groups at 9.50 and 9.44 (see Scheme 1 and Experimental). The ^{13}C NMR spectra show nonequivalence of many pairs of "symmetric" carbon atoms, and the highest value of nonequivalence is observed for the carbon atoms of the azolopyrimidine fragment: $\Delta\delta_{C(2)} = 0.1$ ppm, $\Delta\delta_{C(5)} = \Delta\delta_{C(7)} = 0.06$ ppm, while the chemical shifts for the carbon atoms C(6) and C(6′) are equivalent. Additional NMR experiments gave indirect confirmations for our suggestions. Thus, dilution of the solution of compound **6** in DMSO-d_6 produced no changes of the chemical shifts for the protons of the hydroxy groups, that indicates the presence of stable IMHB. When the spectra were recorded at elevated temperature, the signals for the protons H(2) and H(2′) of the azole rings broadened and became closer. These signals coalesce at 49 °C together with simplification of the spectrum in the region of signals for the oxymethylene protons, indicating an increase of general symmetry of molecules of podand **6**.

Dihydroazolopyrimidine podands were not isolated in none of the dihydro forms because of their strong tendency to oxidation with air oxygen. Macrocyclic product **7** proved the only dihydro derivative stable to oxidation (see Scheme 1), which is stabilized in the 6,7-dihydro form. In turn, the high yields of unsymmetric products **5** and **7** (see Table 1) can indicate that the bulky polyether fragment affects reactivity of terminal groups in compound **1**. It has been noted earlier[24] that molecules of chalcone podand **1** in crystals have a spiral-like geometry with close terminal groups (according to the X-ray diffraction data, the distance between the C_β-atoms of the propenone fragments is 8 Å) in the form of pseudocyclic structure, determined by the *gauche* conformation of the OCH_2CH_2O units (Fig. 4, *a*). Most likely, due to the complexation ability of the polyether chain[13,30] with respect to the molecules of reagent or solvent, such a structure of chalcone podand can be also preserved in solutions. The presence of such a pseudocyclic cavity can hinder access of the reagent molecules to the reaction centers of chalcone podand, coordinating only one of them and thus demonstrating different reactivity of terminal groups of compound **1**. Note that the yields of crownophane **7** depending on the catalyst used indicate that the equilibrium of the reaction in the presence of KOH is significantly shifted to the side of product **7** and, conversely, its yield considerably decreases down to the trace amounts in other cases (see Table 1, *cf.* entries *1*, *2* and *3*, *4*). We have observed analogous dependence earlier in the synthesis of 25-methyl-23,29-diphenyl-8,11,14-trioxa-24-azahexacyclo[20.8.0.0^{2,7}.0^{15,20}.0^{21,26}.0^{25,30}]-triaconta-2,4,6,15(20),16,18,23,28-octaen-27-one.[29] To sum up, the additional intramolecular proximity of the reactive terminal groups in molecules of compound **1** can be due to both the *gauche*-effect from the polyether fragment of the chalcone podand and the template effect of potassium ions resulting from the complexation with the ligand. Note that when a polar protic solvent, ethanol, was used, whose molecules can provide additional stabilization of such complexes, the yield of the macrocyclic product increased. A concerted action of aforementioned effects provides high regioselectivity of the crownophane **7** formation process, which can follow the two possible sequences of cascade reactions (Scheme 2).

Path *A* (see Scheme 2) consists of a cascade of reactions including intermolecular and intramolecular Michael additions (intermediates **8** and **9**) and cyclization in the final step of the synthesis to furnish compound **7**. In turn, path *B* leads to the unsymmetric dihydropyrimidine podand **10** through the intermolecular Michael addition and cyclocondensation. Further intramolecular addition at the β-carbon atom of the propenone fragment[34] of the neighboring terminal group in the intermediate **10** leads to β-adduct **7**.

The formation of crown ether **11** (see Ref. 29) as a result of the reaction of chalcone podand **1** with urea under conditions of alkaline catalysis (KOH) (Scheme 3) can be an argument in favor of the cascade mechanism *A*. In addition, the structural similarity (X-ray diffraction data) of crownophanes **7** and **11** is obvious and comes to the

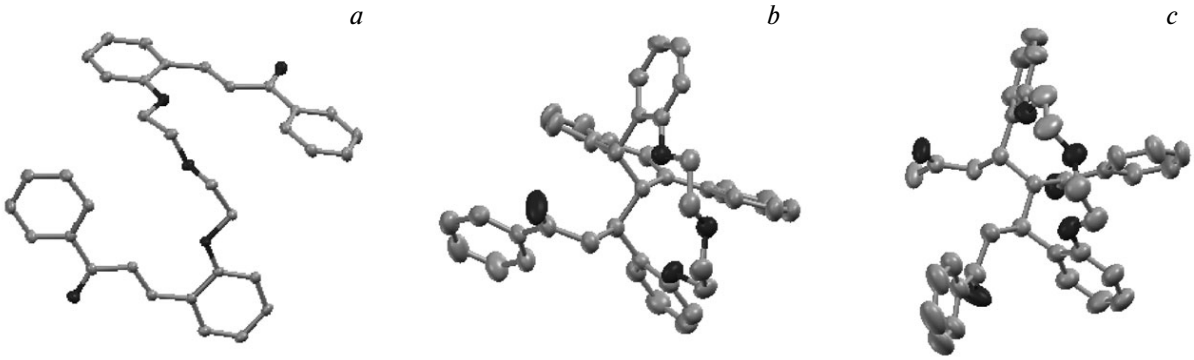

Fig. 4. Molecular geometry of chalcone podand **1** (*a*) and crownophanes **7** (*b*) and **11** (*c*) (according to the X-ray diffraction study).

Scheme 2

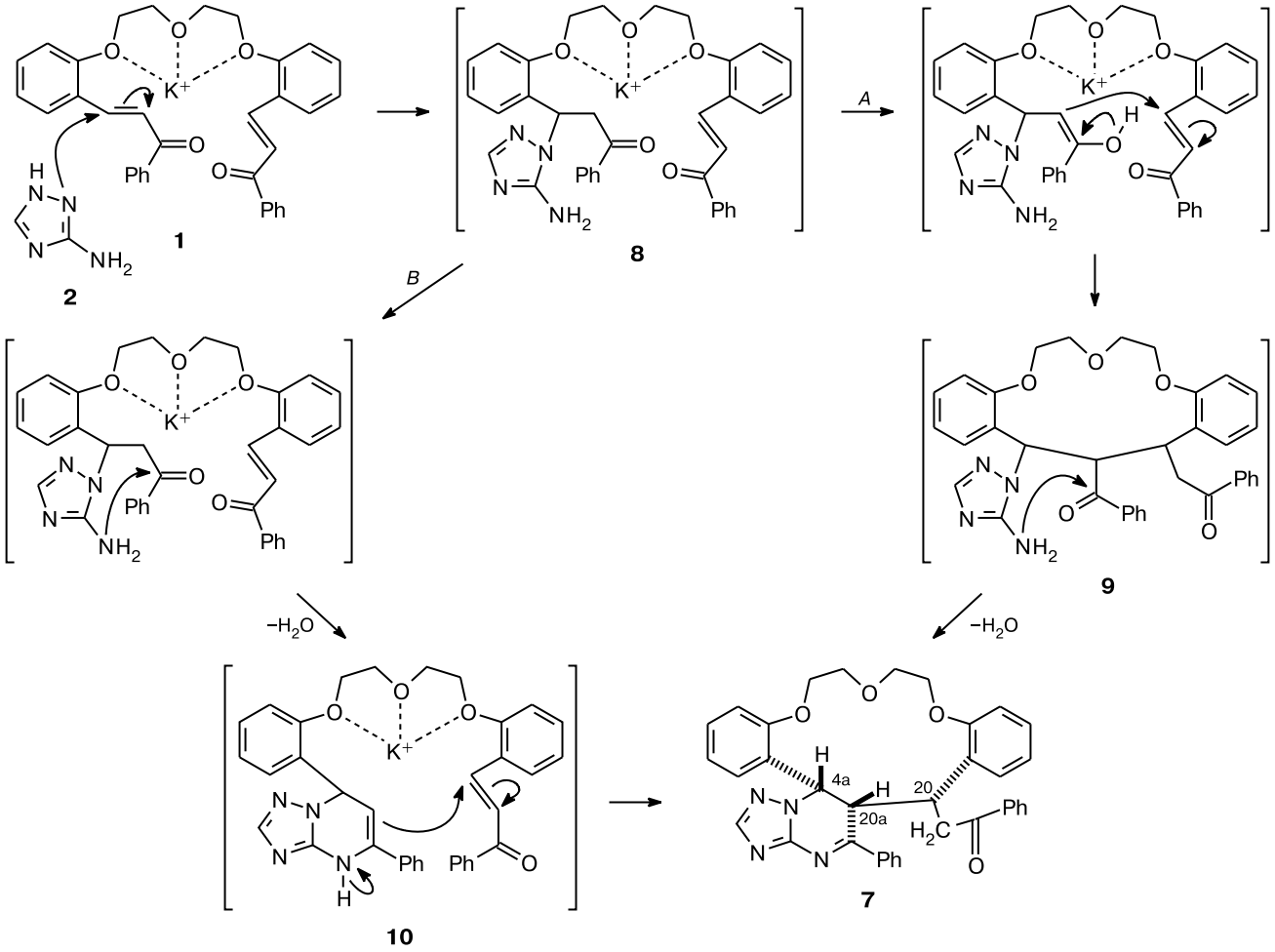

same space geometry of the polyether fragment with identical $a—g^{(+)}—a—a—g^{(-)}—a$ sequence of the oxyethylene units (Fig. 4, *b*, *c* and 5). The angle (121.57°) between the mean-square planes, passing through the atoms C(20)—C(15) and C(26)—C(21) of the phenoxy substituents in compound **7**, virtually coincides with the analogous angle in crownophane **11**. Stereoisomerism of the aliphatic fragment C(4a)—C(20a)—C(20) in crownophane **7** (see Scheme 2) is identical to that of similar fragment in crownophane **11** and differs from that described earlier for the β-adduct with chalcone.[34]

Another indirect confirmation of the initial sequence of intermolecular and intramolecular Michael additions (see Scheme 2, path *A*) can be the antiparallel stereoorientation of the terminal chalcone groups in the starting compound **1**, which is observed in the geometry of crownophanes **7** and **11** (see Fig. 4, *b*, *c*). Such a mutual arrangement of reactive groups of chalcone podand together with the template and *gauch*-effects, most likely, provides the high stereoselectivity of the formation of molecules of only one stereoisomer **7** (racemate) with three asymmetric centers C(35), C(34), C(33) with the relative configuration *rac*-(35*S**,34*R**,33*S**) (the numeration is given as in the X-ray diffraction data).

The ^{1}H NMR spectra of crownophane **7** are characterized by an unusually high-field shifts for the protons H(20) and H(5) in the region δ 3.16 and 5.59, respectively (Fig. 6), that is explained by the shielding effect of the triazolo-

Scheme 3

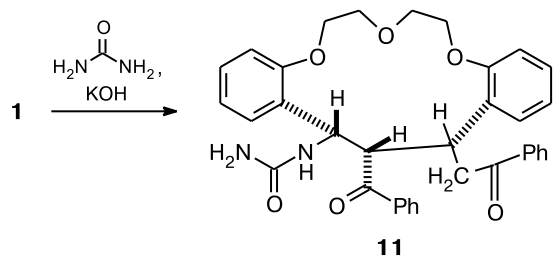

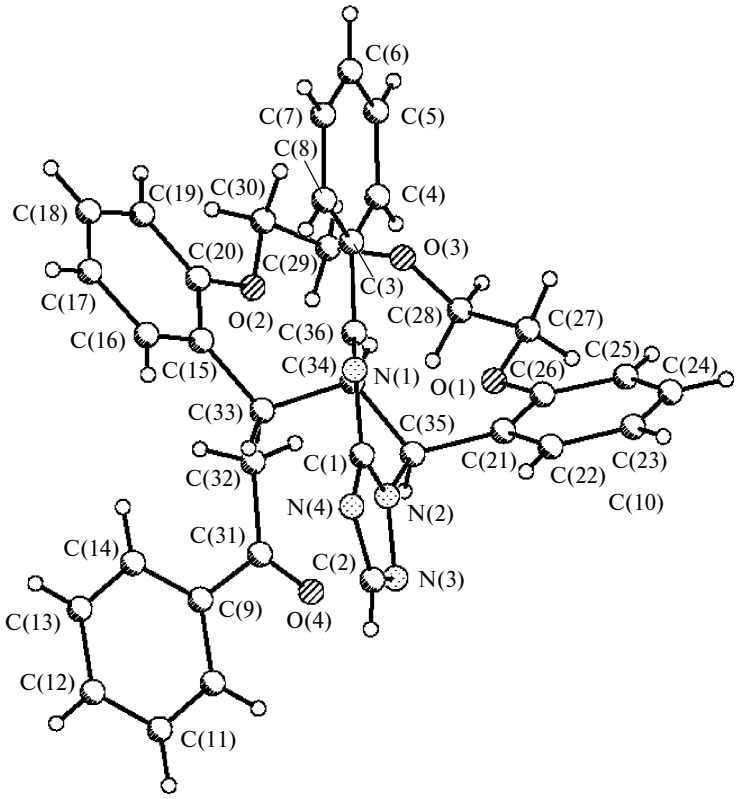

Fig. 5. Molecular geometry of crownophane **7** (according to the X-ray diffraction study).

pyrimidine ring. According to the X-ray diffraction data, the distances between the hydrogen atom H(20) and H(5) and the plane of the condensed ring are 2.25 and 2.40 Å, respectively, and these both atoms are placed inside the cone of magnetic anisotropy. It is probable, that this conformation is also preserved in solution, that is confirmed by the presence of the cross-peak between the H(5) and H(2) in the ^{1}H—^{1}H NOESY 2D spectrum.

In conclusion, in the present work we studied effects of such factors as the nature of catalyst, solvent, and spatial geometry of the starting chalcone podand on the selectivity of cyclocondensation process and degree of oxidation of triazolopyrimidine podands. We also showed the role of potassium ions present in the reaction medium, which coordinate with oligooxyethylene cavity of the molecule of chalcone podand and provide additional intramolecular proximity of their terminal groups, thus shifting the equilibrium to the side of intramolecular Michael addition. These cascade transformations result in the formation of stable 6,7-dihydro-1,2,4-triazolo[1,5-*a*]pyrimidine crownophane in form of only one diastereomer with three asymmetric centers C(35), C(34), C(33) of relative con-

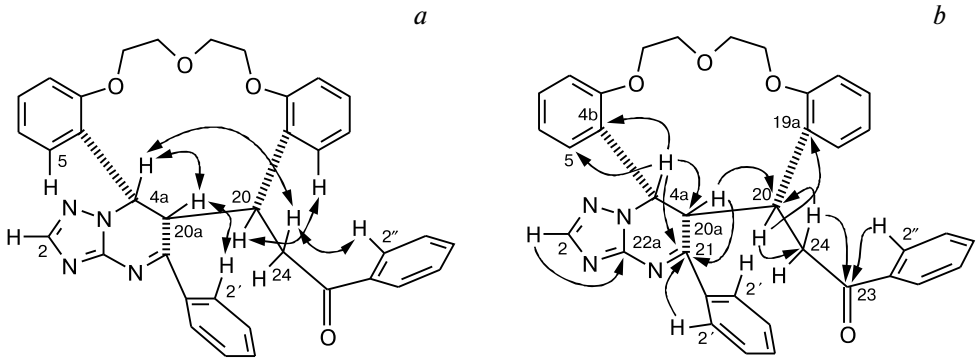

Fig. 6. Stereoorientation of hydrocarbon skeleton C(4a)—C(20a)—C(20)—C(24) in crownophane **7** and selected correlations observed in the ^{1}H—^{1}H NOESY (*a*) and ^{1}H—^{13}C HMBC (*b*) 2D spectra.

figuration *rac*-(35*S**,34*R**,33*S**) (the numeration is given as in the X-ray diffraction data).

Experimental

IR spectra were recorded on a Spectrum One IR Fourier-spectrometer (Perkin—Elmer) using a diffuse reflectance sampling accessory (DRA). ^{1}H and ^{13}C NMR spectra were recorded on a Bruker DRX-400 spectrometer (400 and 100 MHz, respectively) in DMSO-d_6 relatively to Me_4Si and DMSO-d_6 (δ_C 39.5) as internal standards. Full assignment of signals in the ^{1}H and ^{13}C NMR spectra was performed using two-dimensional experiments COSY, NOESY, HSQC, HMBC. Melting points were measured on a Boetius heating microstage. Reaction progress and purity of compounds were monitored by TLC on Silufol-254 plates, visualized in iodine vapors.

Reversed-phase HPLC was performed on an Agilent 1100 analytic liquid chromatograph, using a LiChrosorb RP-18, LKB, 4.0×250 mm column with the particle sizes 5 μm and temperature of the column 35±1 °C. Water was used as a mobile phase *A*, 60% aqueous acetonitrile — as a mobile phase *B*. Elution was performed as follows: first with the gradient from 0 to 100% phase *B* over 20 min, then the isocratic regime with the mobile phase *B* to 40 min, the rate of solvent flow was 0.8 mL min^{-1}. Samples were injected (10 μL) as solutions in DMF. Detection was performed using a diode matrix detector in the UV range on the wavelength 314 nm.

Chalcone podand **1** was synthesized according to the known procedure.[24]

Reaction of chalcone podand 1 with aminotriazole 2 (general procedure). A mixture of chalcone podand **1** (0.25 g, 0.48 mmol) and 3-amino-1,2,4-triazole (0.09 g, 0.96 mmol) in DMF (10 mL) in the presence of the corresponding catalyst (0.48 mmol of KOH, 0.48 mmol of Et_3N, or 0.06 mL of 1.15 *M* aq. HCl) or without catalyst (see Table 1) was heated at 80 °C for 35 h. Water was added to the reaction mixture, a precipitate formed was filtered off and washed with water several times. Purification and separation of products **3**—**7** were performed by column chromatography (SiO_2), eluting with the benzene—ethyl acetate—*n*-butanol (25 : 25 : 2) solvent system. Products **4** and **7** were isolated from the reaction mixture (DMF or EtOH, see Table 1) in 70% (0.22 g) and 18% (0.05 g) yields, respectively. Products **5** and **6** were isolated from the reaction mixture (DMF, HCl) in 46% (0.15 g) and 22% (0.07 g) yields, respectively. The ratios of **3**—**7** were evaluated using ^{1}H NMR spectra of the reaction mixtures and by the reversed-phase HPLC. Retention times for compounds were as follows: 16.9 min (for **8**), 20.7 min (for **6**), 22.0 min (for **5**), 23.2 min (for **4**), 26.9 min (for **3**), 27.9 min (for **7**).

1,5-Bis[2-(1-(5-phenyl-1,2,4-triazolo[1,5-*a*]pyrimidin-7-yl)phenoxy)]-3-oxapentane (4). M.p. 152—155 °C. ^{1}H NMR, δ: 3.36 (m, 4 H, H(12′)); 3.98 (m, 4 H, H(11′); 7.13 (dd, 2 H, H(3′), *J* = 8.4 Hz, *J* = 1.0 Hz); 7.15 (dd, 2 H, H(5′), *J* = 7.6 Hz, *J* = 7.5 Hz, *J* = 1.0 Hz); 7.45 — 7.52 (m, 6 H, H(9′), H(10′)); 7.55 (ddd, 2 H, H(4′), *J* = 8.4 Hz, *J* = 7.5 Hz, *J* = 1.8 Hz); 7.74 (dd, 2 H, H(6′), *J* = 7.6 Hz, *J* = 1.8 Hz); 7.93 (s, 2 H, H(6)); 8.23 (m, 4 H, H(8′)); 8.55 (s, 2 H, H(2)). ^{13}C NMR, δ: 67.70 (C(11′)); 68.48 (C(12′)); 108.71 (C(6)); 112.89 (C(3′)); 119.09 (C(1′)); 120.46 (C(5′)); 127.57 (C(8′)); 128.94 (C(9′)); 131.09 (C(6′)); 131.16 (C(10′)); 132.57 (C(4′)); 135.98 (C(7′)); 145.73 (C(7)); 155.24 (C(3a)); 155.67 (C(2)); 156.16 (C(2′)); 160.00 (C(5)). IR, ν/cm^{-1}: 689, 703, 762 (arom.); 853, 878, 920, 938, 969, 1029; 1052 (ν^s, C_{arom}—O—C_{alk}); 1113, 1132, 1143, 1168, 1194 (ν^{as}, ν^s, C_{alk}—O); 1254 (ν^{as}, C_{arom}—O—C_{alk}); 1283, 12948, 1379, 1447, 1458, 1491; 1535, 1546, 1579, 1600, 1611, 1618 (ν, C=C, C=N); 2866, 2896, 2936, 2967 (δ, C_{alk}—H); 3077, 3111 (δ, C_{arom}—H). Found (%): C, 70.36; H, 4.76; N, 17.06. $C_{38}H_{30}N_8O_3$. Calculated (%): C, 70.58; H, 4.64; N, 17.34.

5-Phenyl-7-[2-(2-{2-[2-(5-phenyl-1,2,4-triazolo[1,5-*a*]-pyrimidin-7-yl)phenoxy]-ethoxy}ethoxy)phenyl]-1,2,4-triazolo-[1,5-*a*]pyrimidin-6-ol (5). M.p. 197—199 °C (MeCN). ^{1}H NMR, δ: 3.25—3.35 (m, 4 H, H(12′), H(12″)); 3.88—3.97 (m, 4 H, H(11′), H(11″)); 7.08—7.19 (m, 4 H, H(3″), H(3‴), H(5″), H(5‴)); 7.46—7.59 (m, 9 H, H(6‴), H(4″), H(4‴), H(9″), H(9‴), H(10″), H(10‴)); 7.76 (dd, 1 H, H(6″), *J* = 7.6 Hz, *J* = 1.6 Hz); 7.99 (s, 1 H, H(6)); 8.02 (m, 2 H, H(8‴)); 8.28 (m, 2 H, H(8′)); 8.36 (s, 1 H, H(2′)); 8.56 (s, 1 H, H(2)); 9.42 (s, 1 H, OH). ^{13}C NMR, δ: 67.79, 67.85 (C(11′), C(11″)); 68.51, 68.56 (C(12′), C(12″)); 108.79 (C(6)); 112.97, 113.01 (C(3″), C(3‴)); 116.70 (C(1‴)); 119.19 (C(1″)); 120.51, 120.65 (C(5″), C(5‴)); 127.64 (C(8′)); 128.08 (C(9‴)); 129.03 (C(9″)); 129.54 (C(8‴)); 129.93 (C(10‴)); 131.10 (C(6″)); 131.26 (C(10′)); 131.56 (C(4‴)); 131.97 (C(6‴)); 132.62 (C(4′)); 133.46 (C(7′)); 136.04 (C(7″)); 136.14 (C(7‴)); 138.91 (C(6′)); 145.86 (C(7)); 150.62 (C(3a′)); 155.01 (C(2′)); 155.26 (C(3a)); 155.69 (C(2)); 156.12 (C(5′)); 156.23 (C(2″)); 156.68 (C(2‴)); 160.10 (C(5)). IR, ν/cm^{-1}: 686, 755, 786, 798 (arom.); 825, 852, 923, 1018; 1051 (ν^s, C_{arom}—O—C_{alk}); 1125, 1144, 1172 (ν^{as}, ν^s, C_{alk}—O); 1246 (ν^{as}, C_{arom}—O—C_{alk}); 1277, 1379, 1402, 1449, 1491; 1518, 1536, 1579, 1602, 1612 (δ, C=C, C=N); 2875, 2930 (δ, C_{alk}—H); 3060, 3085 (δ, C_{arom}—H); 3364 (O—H). Found (%): C, 68.96; H, 4.55; N, 16.83. $C_{38}H_{30}N_8O_4$. Calculated (%): C, 68.88; H, 4.53; N, 16.92.

1,5-Bis[2-(1-(6-hydroxy-5-phenyl-1,2,4-triazolo[1,5-*a*]-pyrimidin-6-ol-7-yl)phenoxy)]-3-oxapentane (6). M.p. 204—206 °C (EtOH). ^{1}H NMR, δ: 3.21—3.33 (m, 4 H, H(12′), H(12″)); 3.86—3.98 (m, 4 H, H(11′), H(11″)); 7.10—7.19 (m, 4 H, H(3′), H(3‴), H(5′), H(5‴)); 7.50—7.55 (m, 10 H, H(6′), H(6‴), H(4″), H(4‴), H(9′), H(9‴), H(10′), H(10‴)); 8.03—8.08 (m, 4 H, H(8′), H(8‴)); 8.36, 8.38 (both s, 1 H each, H(2), H(2′)); 9.44, 9.50 (both br.s, 2 H, OH). ^{13}C NMR, δ: 67.86, 67.88 (C(11′), C(11″)); 68.57, 68.59 (C(12′), C(12″)); 113.08 (C(3′), C(3‴)); 116.74 (C(1′), C(1‴)); 120.66 (C(5′), C(5‴)); 128.10, 128.15 (C(9′), C(9‴)); 129.55 (C(8′), C(8‴)); 129.96, 129.98 (C(10′), C(10‴)); 131.54 (C(4′), C(4‴)); 132.00 (C(6′), C(6‴)); 133.55, 133.61 (C(7), C(7′)); 136.16 (C(7′), C(7‴)); 138.91 (C(6), C(6′)); 150.59, 150.63 (C(3a), C(3a′)); 154.93, 155.03 (C(2), C(2′)); 156.20, 156.26 (C(5), C(5′)); 156.73 (C(2′), C(2‴)). IR, ν/cm^{-1}: 699, 751, 797 (arom.); 821, 853, 926, 1022; 1049, 1084 (ν^s, C_{arom}—O—C_{alk}); 1119, 1146, 1175 (ν^{as}, ν^s, C_{alk}—O); 1243 (ν^{as}, C_{arom}—O—C_{alk}); 1277, 1329, 1400, 1449, 1453, 1488; 1518, 1602 (δ, C=C, C=N); 2877, 2935 (δ, C_{alk}—H); 3048, 3085 (δ, C_{arom}—H); 3333 (O—H). Found (%): C, 67.28; H, 4.48; N, 16.46. $C_{38}H_{30}N_8O_5$. Calculated (%): C, 67.25; H, 4.42; N, 16.52.

1-Phenyl-2-(21-phenyl-10,11,13,14,20,20a-hexahydro-4a*H*-dibenzo-[13,14:8,9][1,4,7]trioxacyclotetradecino[11,10-*e*]-[1,2,4]triazolo[1,5-*a*]pyrimidin-20-yl)-1-ethanone (7). M.p. 216—218 °C (MeCN). ^{1}H NMR, δ: 3.16 (ddd, 1 H, H(20), *J* = 11.2 Hz, *J* = 7.3 Hz, *J* = 4.9 Hz); 3.75 (m, 1 H, OCH_2); 3.94—4.15 (m, 6 H, H(24), OCH_2); 4.21, 4.40, 4.51 (all m,

Table 2. Crystal and X-ray diffraction experimental parameters for compounds **4—7**

Parameter	**4**	**5**	**6**	**7**
Molecular formula	$C_{38}H_{30}N_8O_3 \cdot C_4H_{10}O$	$C_{38}H_{30}N_8O_4 \cdot C_4H_{10}O$	$C_{38}H_{30}N_8O_5$	$C_{36}H_{32}N_4O_4$
Molecular weight	720.82	736.82	678.70	584.66
Crystal system	Monoclinic	Monoclinic	Triclinic	Triclinic
Z	4	4	2	2
Space group	$P2_1/n$	$P2_1/c$	$P\bar{1}$	$P\bar{1}$
a/Å	15.872(3)	15.633(2)	9.378(2)	10.459(2)
b/Å	14.484(2)	14.6525(13)	13.577(3)	11.531(3)
c/Å	17.852(3)	17.893(3)	14.025(3)	13.8534(17)
α/deg	90	90	106.77(2)	82.86(15)
β/deg	115.858(17)	115.883(5)	96.456(18)	71.776(14)
γ/deg	90	90	108.691(19)	70.33(2)
V/Å^3	3693.2(11)	3687.6(8)	1577.8(6)	1494.0(5)
d_{calc}/g cm^{-3}	1.296	1.327	1.429	1.300
F(000)	1520	1552	708	616
μ(Mo-$K\alpha$)/mm^{-1}	0.086	0.090	0.098	0.086
Crystal size/mm	0.47×0.26×0.13	0.48×0.43×0.37	0.48×0.32×0.18	0.49×0.27×0.01
Region of scanning, θ/deg	2.68—26.36	2.69—28.30	2.78—28.28	3.00—26.37
Range of h, k, l	$-19 \le h \le 19$, $-16 \le k \le 18$, $-22 \le l \le 20$	$-19 \le h \le 20$, $-7 \le k \le 19$, $-23 \le l \le 23$	$-12 \le h \le 11$, $-18 \le k \le 17$, $-15 \le l \le 18$	$-13 \le h \le 13$, $-14 \le k \le 13$, $-17 \le l \le 17$
Number of measured reflections	23369	35302	12022	12174
Number of independent reflections with $I > 2\sigma(I)$	7195	8941	7423	5831
R_{int}	0.0589	0.0593	0.0247	0.0443
	2299	3216	3027	2403
R-factors on $I > 2\sigma(I)$				
R_1	0.0467	0.0508	0.0449	0.0406
wR_2	0.0573	0.1005	0.0975	0.0356
R-factors on all the reflections				
R_1	0.1953	0.1549	0.1266	0.1361
wR_2	0.0647	0.1119	0.1054	0.0396
Q-factor on F^2	1.005	0.998	1.001	0.939
Residual electron density (min/max)/e Å^{-3}	−0.129/0.159	−0.175/0.275	−0.320/0.241	−0.138/0.150

1 H each, OCH_2); 5.37 (dd, 1 H, H(20a), J = 11.2 Hz, J = 1.0 Hz); 5.59 (dd, 1 H, H(5), J = 7.7 Hz, J = 1.0 Hz); 6.07 (s, 1 H, H(4a)); 6.23 (d, 1 H, H(16), J = 8.2 Hz); 6.46—6.52 (m, 2 H, H(18), H(19)); 6.69 (td, 1 H, H(6), J = 7.7 Hz, J = 1.0 Hz); 6.74 (ddd, 1 H, H(17), J = 8.2 Hz, J = 6.3 Hz, J = 3.0 Hz); 7.06 (tm, 2 H, H(3′), J = 7.7 Hz); 7.13 (dd, 1 H, H(8), J = 8.4 Hz, J = 1.0 Hz); 7.19—7.25 (m, 2 H, H(4′), H(7)); 7.32 (m, 2 H, H(2′)); 7.51 (tm, 2 H, H(3″), J = 7.5 Hz); 7.61 (tm, 1 H, H(4″), J = 7.5 Hz); 7.84 (m, 2 H, H(2″)); 8.24 (s, 1 H, H(2)). ^{13}C NMR, δ: 39.65 (C(24)); 41.59 (C(20)); 41.90 (C(20a)); 54.67 (C(4a)); 65.31, 66.75, 68.50, 68.86 (C(14), C(13), C(11), C(10)); 110.29 (C(16)); 111.84 (C(8)); 119.53 (C(18)); 120.37 (C(6)); 123.74 (C(4b)); 124.81 (C(5)); 127.06 (C(19a)); 127.25 (C(2′)); 127.49 (C(3′)); 127.77 (C(2″)); 128.27 (C(17)); 128.68 (C(3″)); 129.57 (C(7)); 131.06 (C(19)); 131.27 (C(4′)); 133.12 (C(4″)); 136.54 (C(1″)); 136.98 (C(1′)); 151.79 (C(2)); 154.29 (C(22a)); 154.84 (C(8a)); 156.08 (C(15a)); 177.39 (C(21)); 199.55 (C(23)). IR, ν/cm^{-1}: 682, 694, 743, 755, 765 (arom.); 852, 875, 922, 950, 987, 1001; 1056 (ν^s, C_{arom}—O—C_{alk}); 1117, 1135 (ν^{as}, ν^s, C_{alk}—O); 1231, 1245 (ν^{as}, C_{arom}—O—C_{alk}); 1261, 1261, 1356, 1450, 1494, 1515; 1561, 1588, 1600 (δ, C=C, C=N); 1686 (δ, C=O); 2867, 2884, 2930 (δ, C_{alk}—H); 3038, 3063 (δ, C_{arom}—H). Found (%): C, 73.66; H, 5.65; N, 9.56. $C_{36}H_{32}N_4O_4$. Calculated (%): C, 73.97; H, 5.47; N, 9.59.

X-ray diffraction study. Crystals of triazolopyrimidine podands **4—6** were obtained by the slow concentration of their solutions in DMF—butanol (1 : 1), whereas crystals of 6,7-dihydro-1,2,4-triazolo[1,5-*a*]pyrimidine crownophane **7** — of its solution in acetonitrile. X-ray diffraction study of the compounds was performed on a Xcalibur 3 diffractometer with a CCD-detector (ω-scanning, MoKα-irradiation, λ = 0.71073 Å, graphite monochromator, T = 295(2) K). The set of reflections was obtained and processed using the CrysAlis program package.[35] The structures were solved by the direct method and refined by the full-matrix least squares method first in the isotropic and then in the anisotropic approximation on F^2 for all the nonhydrogen atoms using the SHELXS-97 and SHELXL-97 program packages.[36] Some of the hydrogen atoms were found in the differential synthesis and included in the refinement in the isotropic approximation, some were placed in the geometrically calculated positions and refined using the riding model. The main crystallographic data and refinement parameters

for the structures **4**—**7** are given in Table 2. The experimental X-ray diffraction data for the structures **4**—**7** were deposited with the Cambridge Structural Database with the numbers CCDC822574, CCDC822573, CCDC822572, CCDC822571, respectively.

This work was financially supported by the Council on Grants at the President of the Russian Federation (Program of State Support for Leading Scientific Schools of the Russian Federation, Grant NSh-65261.2010.3) and the Presidium of the Ural Branch of the Russian Academy of Sciences (Project Nos 09-P-23-2001, 09-I-3-2004, and 09-P-3-2001).

References

1. F. S. Babichev, B. Kovtunenko, *Khim. Geterotsikl. Soedin.*, 1977, 147 [*Chem. Heterocyclic. Compd.* (*Engl. Transl.*), 1977, **13**, 117].
2. C. F. H. Allen, H. R. Beilfuss, D. M. Burness, G. A. Reynolds, J. F. Tinker, J. A. VanAllan, *J. Org. Chem.*, 1959, **24**, 787.
3. T. Yasuda, T. Iwamoto, M. Ohara, S. Sato, *Jpn. J. Pharmacol.*, 1999, **79**, 65.
4. G. F. Yang, R. F. Lu, X. N. Fei, H. Z. Yang, *Chin. J. Chem.*, 2000, **18**, 435.
5. K. E. Tahir, H. A. Khamees, S. M. Bayomi, *Boll. Chim. Farm.*, 1995, **134**, 604.
6. I. Sato, Y. Shimoji, H. Fujita, H. Nishino, H. Mizuno, S. Kobayashi, S. Kumakura, *J. Med. Chem.*, 1980, **23**, 927.
7. F. Luque, C. Fernandez-Ramos, E. Entrala, M. J. Rosales, M. C. Salas, J. Navarro, M. Sanchez-Moreno, *Toxicol. in Vitro*, 2000, **14**, 487.
8. J. A. R. Navarro, J. M. Salas, M. A. Romero, R. Vilaplana, F. Gonzalez-Vilchez, R. Faure, *J. Med. Chem.*, 1998, **41**, 332.
9. M. E. Fraley, R. S. Rubino, W. F. Hoffman, S. R. Hambaugh, K. L. Arrington, R. W. Hungate, M. T. Bilodeau, A. J. Tebben, R. Z. Rutledge, R. L. Kendall, R. C. McFall, W. R. Huckle, K. E. Coll, K. A. Thomas, *Bioorg. Med. Chem. Lett.*, 2002, **12**, 3537.
10. S. Selleri, F. Bruni, C. Costagli, A. Costanzo, G. Guerrini, G. Ciciani, B. Costa, C. Martini, *Bioorg. Med. Chem.*, 1999, **7**, 2705.
11. J. M. Salas, M. A. Romero, M. P. Sánchez, M. Quirós, *Coord. Chem. Rev.*, 1999, **193**—**195**, 1119.
12. S. Orihuela, M. P. Sánchez, M. Quirós, J. Molina, R. Faure, *J. Mol. Structure*, 1997, **415**, 285.
13. *Host Guest Complex*: *Chemistry, Macrocycles, Synthesis, Structures, Applications*, Eds F. Vögtle, E. Weber, Springer-Verlag, Berlin, 1985, 421 pp.
14. S. M. Desenko, *Khim. Geterotsikl. Soedin.*, 1995, 147 [*Chem. Heterocycl. Compd.* (*Engl. Transl.*), 1995, **31**, 125].
15. V. D. Orlov, S. M. Desenko, K. A. Potekhin, Yu. T. Struchkov, *Khim. Geterotsikl. Soedin.,* 1988, 229 [*Chem. Heterocycl. Compd.* (*Engl. Transl.*), 1988, **24**, 192].
16. S. M. Desenko, V. D. Orlov, *Khim. Geterotsikl. Soedin.*, 1989, 1071 [*Chem. Heterocycl. Compd.* (*Engl. Transl.*), 1989, **25**, 894].
17. S. M. Desenko, V. D. Orlov, V. V. Lipson, *Khim. Geterotsikl. Soedin.*, 1990, 1638 [*Chem. Heterocycl. Compd.* (*Engl. Transl.*), 1990, **26**, 1362].
18. S. M. Desenko, Kh. Estrada, V. D. Orlov, O. A. Ponomarev, *Khim. Geterotsikl. Soedin.*, 1991, 105 [*Chem. Heterocycl. Compd.* (*Engl. Transl.*), 1991, **27**, 88].
19. V. V. Lipson, S. M. Desenko, V. D. Orlov, M. N. Shirobokova, V. N. Chernenko, L. I. Zinov´eva, *Khim. Geterotsikl. Soedin.,* 2000, 1542 [*Chem. Heterocycl. Compd.* (*Engl. Transl.*), 2000, **36**, 1329].
20. R. V. Rudenko, S. A. Komykhov, V. I. Musatov, S. M. Desenko, *J. Heterocycl. Chem.*, 2009, **46**, 285.
21. S. M. Desenko, E. S. Gladkov, N. V. Getmanskii, I. M. Zemlin, V. D. Orlov, *Khim. Geterotsikl. Soedin.,* 1999, 678 [*Chem. Heterocycl. Compd.* (*Engl. Transl.*), 1999, **35**, 608].
22. C. M. Desenko, V. D. Orlov, V. V. Lipson, O. V. Shishkin, K. A. Potekhin, Yu. T. Struchkov, *Khim. Geterotsikl. Soedin.*, 1993, 109 [*Chem. Heterocycl. Compd.* (*Engl. Transl.*), 1993, **29**, 95].
23. C. M. Desenko, E. S. Gladkov, S. A. Komykhov, O. V. Shishkin, V. D. Orlov, *Khim. Geterotsikl. Soedin.,* 2001, 811 [*Chem. Heterocycl. Compd.* (*Engl. Transl.*), 2001, **37**, 747].
24. I. G. Ovchinnikova, O. V. Fedorova, P. A. Slepukhin, I. A. Litvinov, G. L. Rusinov, *Kristallografiya*, 2009, **54**, 32 [*Crystallogr. Rep.* (*Engl. Transl.*), 2009, **54**, 31].
25. I. G. Ovchinnikova, O. V. Fedorova, E. G. Matochkina, M. I. Kodess, P. A. Slepukhin, G. L. Rusinov, *Izv. Akad. Nauk, Ser. Khim.*, 2009, 1150 [*Russ. Chem. Bull., Int. Ed.*, 2009, **58**, 1180].
26. M. S. Zhidovinova, O. V. Fedorova, G. L. Rusinov, I. G. Ovchinnikova, *Mol. Diversity*, 2003, **6**, 323.
27. A. N. Levov, Le Tuan An´, A. I. Komarova, V. M. Strokina, A. T. Soldatenkov, V. N. Khrustalev, *Zh. Org. Khim.*, 2008, **44**, 457 [*Russ. J. Org. Chem.* (*Engl. Transl.*), 2008, **44**, 456].
28. Le Tuan An´, A. N. Levov, A. T. Soldatenkov, R. D. Gruzdev, Chyong Khong Khieu, *Zh. Org. Khim.*, 2008, **44**, 463 [*Russ. J. Org. Chem.* (*Engl. Transl.*), 2008, **44**, 462].
29. I. G. Ovchinnikova, O. V. Fedorova, E. G. Matochkina, I. M. Kodess, A. A. Tumashev, P. A. Slepukhin, G. L. Rusinov, V. N. Charushin, *Makrogeterotsikly* [*Macroheterocycles*], 2010, **3**, 108 (in Russian).
30. E. Weber, J. L. Toner, I. Goldberg, F. Vögtle, D. A. Laidler, J. F. Stoddart, R. A. Bartsch, C. L. Liotta, in *Crown Ethers and Analogs*, Eds S. Patai, Z. Rappoport, John Wiley and Sons, Chichester, 1989, p. 3.
31. I. Azumaya, K. Yamaguchi, I. Okamoto, H. Kagechika, K. Shudo, *J. Am. Chem. Soc.*, 1995, **117**, 9083.
32. W. L. Meyer, P. B. Meyer, *J. Am. Chem. Soc.*, 1963, **85**, 2170.
33. S. Toyota, T. Makino, *Tetrahedron Lett.*, 2003, **44**, 7775.
34. V. V. Lipson, I. V. Ignatenko, S. M. Desenko, O. V. Shishkin, S. A. Komykhov, N. V. Logvinenko, V. D. Orlov, H. Meier, *J. Heterocycl. Chem.*, 2003, **40**, 1081.
35. *CrysAlis Pro, Version 171.33.66*, Oxford Diffraction, Ltd.
36. G. M. Sheldrick, *Acta Crystallogr.*, *Sec. A: Found Crystallogr.*, 2008, **64**, 112.

Received November 26, 2010;
in revised form February 28, 2011